Abstract

Recent laboratory studies focusing on multigenerational approach demonstrated drastic phenotypic effects after chronic fish irradiation exposure. No irradiation effect at phenotypic scale was observed for F0 (reproductive performances) while early mortality and malformations were observed in F1 offspring whether they were irradiated or not. The objective was to study molecular mechanisms likely to be involved in these phenotypic effects induced by parental irradiation. Thus, F0 adult zebrafish were irradiated for ten days until reproduction and maternal involvement in offspring development was assessed. Levels of maternal provided cortisol and vitellogenin, needed for embryo development, were not impacted by irradiation. However, maternal transcriptome highlighted irradiation effect on processes involved in oocyte development, as well as on essential maternal factors needed for offspring development. Therefore, this study highlighted the importance of parental exposure on offspring fate and of the importance of multigenerational exposure in risk assessment.

Keywords: multigenerational, maternal transcripts, cortisol, vitellogenin, zebrafish, irradiation

Altered ovarian transcriptome is linked to early mortality and abnormalities in zebrafish embryos after maternal exposure to gamma irradiation

Guirandy Noëmie[a*], Armant Olivier[a], Frelon Sandrine[a], Pierron Fabien[b], Geffroy Benjamin[c], Daffe Guillemine[b], Houdelet Camille[c], Gonzalez Patrice[b], Simon Olivier[a]

[a] IRSN/PSE-ENV/SRTE/LECO, Centre de Cadarache-B.P. 3 – Bat 183 – 13115 St Paul Lez Durance, France

[b] Univ. Bordeaux, CNRS, EPOC, EPHE, UMR 5805, F-33600 Pessac, France

[c]MARBEC, Univ Montpellier, CNRS, Ifremer, IRD, Palavas-Les-Flots, France

[*]Corresponding author.

E-mail addresses: noemie.guirandy@hotmail.fr

1. Introduction

As aquatic ecosystems are particularly impacted by chemical pollutants, many data are available on their phenotypic effects and toxic mechanisms of action. Recently, multigenerational consequences of chemical exposure is a growing area of interest for environmental risk assessment (ERA). Although nuclear accidents such as Chernobyl and Fukushima represent an ecological threat for wildlife populations, much less is known regarding the effects of ionizing radiations (IR) over generations (Beresford et al., 2020; Car et al., 2022; Cunningham et al., 2021; Geras'kin et al., 2021).

We previously showed that laboratory exposure of adult zebrafish to high dose rate (50 mGy.h-1, 12 Gy) for 10 days did not alter their reproductive performances nor survival (Guirandy et al. 2019). But it is likely that effects would be more tenuous since

DNA damages and oxidative stress were already detected following IRs exposure (Simon et al., 2011). Moreover, these subtle effects could be maternally transmitted, with potential consequences on offspring fitness. We indeed reported that the irradiated or non-irradiated (recovery condition) offspring from irradiated genitors at a high dose rate showed a high mortality from 24 hours post fertilization (hpf) (Guirandy et al., 2019). Similar results were observed by Hurem et al. 2017 after an exposition to 53 mGy.h-1, which induced non-viable offspring. Another study at a lower dose rate (5 mGy.h-1, 30d, 3.6 Gy) showed an impact of IR on the irradiated or non-irradiated offspring leading to high mortality rates at early stages of development (8 days post fertilization (dpf)) as well as male-biased sex ratio at adulthood (Guirandy et al., 2022). All these studies highlighted a high mortality of the offspring from irradiated parents. The mechanisms of parental effect on offspring still remain unclear.

Strong maternal effects are likely to occur following exposure to IRs since mothers not only provide genomic material but also many essential cytoplasmic components and mRNA needed to achieve the proper embryonic development of the offspring. First, females contain the future eggs, on which IR may induce oxidative stress and DNA damages (Guirandy et al., 2019; Hurem et al., 2018, 2017). Damaged eggs would then suffer higher mortality, as observed by Chen et al. 2015 and Vuori et al. 2008. Secondly, some essential macro-molecules are provided by female and are needed for embryo development (“Maternal Effect Genes in Development, Volume 140 - 1st Edition,” n.d.). Two macro-molecules are of particular interest, namely vitellogenin (VTG) which needs to be cleaved by cathepsin D in order to form the yolk egg (Finn, 2007; Yilmaz et al., 2018); and cortisol (the main stress hormone in fish (Sadoul and Geffroy, 2019)). VTG is the yolk egg precursor and the developing offspring of oviparous animals are entirely dependent on this energy store. A defect in VTG

quantity or in its metabolism is known to be a cause of early mortality (Soares et al., 2009; Yilmaz et al., 2018). Altered cortisol concentration could also play a key role in the described effects since a proper maternally-provided quantity of cortisol is needed for early embryo development (Faught and Vijayan, 2018; McCormick, 1999; Nesan and Vijayan, 2016, 2012). Finally, maternal mRNAs support embryonic development until activation of the zygote genome (Abrams and Mullins, 2009; “Maternal Effect Genes in Development, Volume 140 - 1st Edition,” n.d.). Indeed, good quality eggs production begins with oocyte development in females. For instance, many studies highlighted the primordial role of maternal mRNAs and more generally of the Balbiani body (Bb) in embryo axis establishment and progeny survival (Abrams and Mullins, 2009; Flores et al., 2008; Langdon and Mullins, 2011). Particularly, formation of the Bb in developing oocytes allows establishment of the first polarity (animal/vegetal) of embryo (Jamieson-Lucy and Mullins, 2019; Marlow, 2010). Two maternal genes are particularly involved in Bb formation; (i) buc, which allows Bb assembly and (ii) macf1, which allows Bb translocation and dispersal in oocyte. Maternal mRNA needed later for embryo development are accumulated in the Bb before to be dispersed to their functional localization.

Here, we assessed maternally transmitted effects following parental exposure to gamma irradiation with no offspring irradiation (recovery) as well as irradiation of both genitors and offspring (irradiated). Maternal transcriptome was then analysed to get mechanistic insights into the impact of irradiation. This study represents a first step to define parental effects after irradiation, by assessing mother involvement. Hence, after a gamma irradiation performed at 50 mGy.h-1 for 10 days, we sampled ovaries and eggs to study irradiation-induced impacts (i) on maternally deposited material through cortisol and VTG measurements, (ii) on oocyte development and (iii) on specific

maternal transcripts needed for offspring development by analysing ovary transcriptome (RNA-Seq) in order to get insights into the mechanisms that could explain the transmitted effects from female to offspring. 50 mGy.h-1 dose rate was used to underspin effects observed in our previous study and to assess a mechanistic study at high dose rate not observed in the environment.

2. Materials and methods

2.1. Fish husbandry

The project (APAFIS#15821) was authorized by the Institut de Radioprotection et de Surêté Nucléaire ethics committee no. 81 (EU 0520) in an application under the directive 2010/63/UE relating to animal care. The study was conducted on AB strain zebrafish that were kept, reproduced, and irradiated in a zebrafish housing system (Zebtec Tecniplast Stand Alone) with recirculating oxygenated freshwater. Adult fish were acclimatized over 3 weeks to tap water + 20% demineralized water renewed daily (Aquadem; pH 7.4 ± 0.2, conductivity $= 398 \pm 2\ \mu S\ cm^{-1}$, temperature $= 28.4 \pm 0.3\ °C$), with a 12:12-h light:dark cycle photoperiod. The fish were fed ab libitum three times a day with GEMMA Wean (Skretting®).

2.2. Adult and embryo exposure

Nominal dose rate was $50\ mGy.h^{-1}$ for the irradiated condition. Gamma-rays were emitted from a 137Cs source (444 GBq, 662 keV; Institut de Radioprotection et de Surêté Nucléaire MICADO-Lab platform). Dose rate was simulated using MCNP5 software and measured using thermoluminescent dosimeters (Chiyoada Technologies), and the values represented between 80 and 120% of the nominal values. Control condition was kept in a separate room ($60–80\ nGy.h^{-1}$). The population density of adult fish was $0.7\ L.g^{-1}$.

Twenty-four adult fish per condition (12 females : 12 males) were irradiated over 10 d. Daily controls and feeding were conducted as described in Guirandy et al., 2019.

F1 offspring were obtained from 12 F0 spawning couples (24 fish, 1 female:1 male) (i.e., replicates) per condition. Mating and eggs viability were determined as described in Guirandy et al., 2019. The 3hpf-embryos from 6 spawns per condition were separated into 2 groups of 30 eggs per clutch. The first one F1 embryos were then positioned in an incubator and irradiated at 50 $mGy.h^{-1}$ (irradiated) (Figure 1). The second group was placed in non-irradiated incubator (recovery). F1 embryos were maintained in both conditions over 6days. The same culture medium was used for embryos and adults and 10% was replenished daily.

F0 adults were then placed in control condition and reproduction was done as explained before, at 6 days (resilience_6d) and 36 days (resilience_36d). Each F1 obtained offspring were kept in control conditions for 4 days.

2.3. Ecological endpoints and morphological analysis

Reproductive performances (reproductive success, fecundity: number of eggs laid per female) of adults were measured after 10 days of exposure.

The progeny survival rate was assessed from 24 to 96 hours post fertilization (hpf) in the control, irradiated, and non-irradiated (recovery) conditions (30 eggs from 6 spawns per condition).

Photographs of F1 larvae were recorded at 72hpf (6 to 30 larvae per condition) under a stereomicroscope (Nikon SMZ800) connected to a high-resolution camera (acA1300-60gm, Basler, Germany). Recording was performed using Media Recorder Software (v.4.0.542.1, Noldus Information Technology, Netherlands) and the analysis of photos was performed using the DanioScope Software (v.1.1.110, Noldus

Information Technology, Netherlands) in order to assess morphology measurements (surface of yolk reserve) and malformations (cardiac edema). Analyses were made for F1 irradiated, F1 recovery, F1 resilience 6d and F1 resilience 36d.

2.4. Sequencing library and transcriptomic analysis of ovaries

Ovaries were dissected after reproduction and gonads were kept in RNALater® (Sigma-aldrich) at -80°C until analysis. RNA extractions were made from female gonads (8 per condition). Each sample was homogenized in 600 µL of ice-cold RTL buffer (Qiagen) with 6 µL of β-mercaptoethanol using a tissue homogenizer for 3 times 15s Following centrifugation, DNA and RNA were extracted from the homogenate using the AllPrep DNA/RNA kit (Qiagen) according to manufactures' guidelines, with DNAseI's treatment (Qiagen) according to the manufacturer's recommendations.

Libraries were generated from 1 µg of total RNA following the TruSeq mRNA stranded protocol (Illumina). RNA integrity (RIN) assessed using RNA Nano Chips (Bioanalyzer 2100, Agilent) did not show any sign of degradation (RIN > 7). Librarie quality and concentration were measured on DNA1000 Chips (Bioanalyzer 2100, Agilent) and sequenced on a NovaSeq 6000 platform to produce 50 bases long paired-end reads (Clinical Research Sequencing Platform, Broad Institute, MIT, Cambridge, USA). Good-quality reads (Q > 30) were produced for each sample (Table S1). Quality check of paired end reads and quantification of the RNAseq data were performed as described before (Murat El Houdigui et al., 2019). Briefly, read quality was assessed with FastQC (https://www.bioinformatics.babraham.ac.uk/projects/fastqc/), adapter sequences were removed with TrimGalore! v0.6.4 (http://www.bioinformatics.babraham.ac.uk/projects/trim_galore/) and mapped against the GRCz11 zebrafish reference genome using RNA-STAR v020201 and the known exon–exon junctions from Ensembl release 103. Normalisation and differential

expression analysis were performed with DESeq2 v1.26.0. Genes with adjusted p-value < 0.05 (false discovery rate) were considered as differentially expressed in all analysis (DEG). Genes with |log2FoldChcange| ≥ 1 and adjusted p-value < 0.05 (false discovery rate) were considered as up or down regulated.

2.5. Enrichment analysis

ClusterProfiler, a R package, was used to perform pathway enrichment using Gene ontology terms (GO terms), Kyoto Encyclopedia of Genes and Genomes pathway (KEGG pathway) on the DEG obtained from DESeq2 (Table S2). Enrichments with p-value from Fisher's exact test ≤ 0.05 were considered significant. Dot plots were produced using the R package ggplot2.

2.6. RT-qPCR analysis

RNA extraction for qPCR was performed as for the RNA-seq. A total of 1 µg of RNA was used to synthesize first-strand cDNA using the GoScript Reverse Transcription System (Promega), according to the manufacturer's guidelines. cDNA was then diluted 40-fold. Real-time PCR reactions were then performed in a thermocycler (LC480, Roche; 95 °C for 2 min, followed by 45 cycles of 95 °C for 15 s and 60 °C for 1 min). Each 15 µL reaction contained 7.5 µL of GoTaq qPCR master mix (Promega), 5 µL template and the specific primer pairs at a final concentration of 0.33 µM each. Amplification efficiencies for all primer sets were calculated to allow direct comparison of amplification plots according to the ΔΔCt method (Livak and Schmittgen, 2001). Relative quantification of gene expression was achieved by amplification of endogenous control genes chosen from our RNAseq dataset, i.e. genes for which their transcription level was not impacted by irradiation (*aspa*, *pdia6*). During our experiment, total RNAs were quantified and the same quantity was used to be reverse-

transcribed. During the subsequent qPCR amplifications, the output cycles of the endogenous controls were examined, no significant difference was observed on the output cycle of aspa and pdia6 among conditions. The mean Ct value of the two latter genes was used as reference. Primers used are available in Table S3 and are involved in oogenesis and sex determination. Log2FC from RNAseq and qPCR analysis were compared in order to validate RNAseq data (Figure S1); they varied similarly between the two analyses.

2.7. Steroid extraction and cortisol measurement

A half female's gonad per replicate was flash-frozen in liquid nitrogen and kept at -80°C until extraction. Gonads were then thawed and transferred in sodocalcic glass tube. 1ml of ethyl acetate/cyclohexane (50:50) was added per sample before grinding for 2 min in a potter (Eurostardigital, IKA Labortechnik,) at 2000 Tr/min. Lysate was then transferred to new sodocalcic glass tube. This step was carried out twice in order to recover a maximum of material as recommended in Sadoul and Geffroy, 2019. Tubes were vortexed for 10 sec then centrifuged for 5 min at 5000G. Supernatant was collected in a sodocalcic glass tube. This step was performed twice. Each sample was evaporated to dryness under nitrogen at 40 °C and resuspended in buffer from the "Cortisol Express ELISA Kit" from Cayman Chemical. Cortisol assay were then performed according to manufacturer's guidelines.

2.8. Protein extraction and VTG western blot analysis of 24hpf eggs

Twenty 24hpf-eggs per replicate were quick frozen in liquid nitrogen and stored at -80°C until extraction. For protein extraction, samples were placed in a modified RIPA lysis buffer (Sigma Aldrich; with anti-protease mixture), with 0.5-mm diameter zirconium beads and homogenized by three 5000-rpm cycles at 4°C in a Precellys

grinder system (Ozyme). After 30mn incubation on ice, crude extracts were centrifuged for 10 minutes at 4°C at 5000g. Protein concentration was determined using the BCA kit (Thermo Scientific) with BSA as a standard, according to the manufacturer's instructions and then adjusted to a same concentration to ensure the loading of the same amount of proteins for western blot analysis. After denaturation (15mns, 95°C with Laemli buffer (Tris (0,31M), DTT (0,25M), BBP (0,02%), SDS (10%) and glycerol) 9µg of proteins from each sample were loaded in precast gels (4-20%? TGX Biorad) and electrophoresis was run in TGS buffrer during 50min (80V for 15 min and 150V 35min). 5µL of load marker (RNP800E, ECL Plex Fluo rainbow) were added in one well. After migration, gel was transferred on a polyvinylidene fluoride (PDVF, GE Healthcare) membrane (1h, 4°C, transfer buffer (TGS 1X, ethanol (20%)), for 1 hours at 100V. Membrane was then blocked with BSA 1% (TBST-BSA buffer (TBS1X, pH=7.5 – Tween 0.1% - 1% filtered BSA) for 1hand incubated overnight at 4°C in primary mouse antibody JE-10D4 (Abcam ab36804, dilution 1:1000 in TBST-BSA) followed by incubation in secondary anti-mouse antibody Cy5® (Goat Anti-Mouse IgG H&L preadsorbed (ab6563)dilution 1:6000 in TBST-BSA) for 2h at 4°C. Membrane was finally rinsed and results were visualized with Typhoon FLA 9500 (GE Healthcare) at 670nm, PMT ().Integrations of bands (volume without background) were done using ImageQuantTL software (1D gel analysis module). Recent bibliography shows that the use of housekeeping protein to normalization is difficult (Eaton et al., 2013; Moritz, 2017). These findings were proved in our case with traditional proteins (β-actin and α-tubulin) which were highly impacted by gamma irradiation (Figure S2). Reproducibility of lane was proved by multiple gel migrations, as described by (Eaton et al., 2013; Moritz, 2017; Richon et al., 2000), using total protein gel stained in parallel (Table S4*)* since the use of housekeeping protein to normalization is difficult after exposure to a

stressor (Eaton et al., 2013; Moritz, 2017). Homogeneity of variances was tested using bartlett's test for each membrane (*p-val>0.05*) and variances of two gels were tested using Anova (*p-value>0.05*).

2.9. Statistical analysis

For F1 survival rate, F1 morphology, F1 maturation products of vitellogenin intensity and F0 cortisol concentrations, data were presented as mean values ± SE, with significance taken as $p < 0.05$. For F1 vitellogenin ratio, results were presented by the ratio 30kDa band/ 26kDa band. Concerning data relating to the F1 generation (survival rate and vitellogenin ratio), conditions were compared using a GLM (Generalized Linear Model, glm function in R) with binomial distribution. Concerning data related to morphology, vitellogenin density results and cortisol, conditions were compared using Anova with BoxCox transformation when normality and homogeneity were not verified. A TukeyHSD, post-hoc test, was then used. Concerning qPCR data, data were presented as log2FoldChange where FoldChange (FC) = (mean $2^{-\Delta Ct_{irradiated}}$ - mean $2^{-\Delta Ct_{control}}$)/ mean $2^{-\Delta Ct_{control}}$. Conditions were compared using Anova with BoxCox transformation when normality and homogeneity were not verified. A Tukey (HSD), post-hoc test, was then used. When normality was not verified even after data transformation, a non-parametric test was used (kruskal wallis). A Dunnet test with Bonferroni correction was then used as post hoc test.

The analyses were performed using R software (R Core Team, 2021) with the following packages : "tidyverse", "here", "knitr", "lme4", "MASS","car". Figures were produced using the package "ggplot2".

3. Results

3.1. F0 reproductive performances and F1 survival

F0 adult fish (n=24 per condition) and F1 embryos (n=30 eggs X 6 spawns per condition) were irradiated to a cumulative dose of 12Gy and 4.8Gy, respectively. The direct exposure to IRs did not induce F0 adult mortality over the experiment. The reproductive success (RS) of F0 irradiated adults was lower (n=12 mating pairs, 75%), but not significantly different to control fish (n=12, 92%). No effect on fecundity was observed after exposure to gamma irradiation (n=9, 367±170), compared to the control group (n=11, 344±153).

At 24 hpf, the percentage of F1 mortality for control, irradiated and recovery groups reached 54.9%±5.6, 71.7%±10.7 and 77.0%±7.0, respectively (Figure 2). Despite enhanced mortality for both irradiated and recovery conditions, no significant difference was observed compared to the control group. However, an important variability was observed for all groups. The same trend was observed at 48 hpf (control: 56.1%±5.9; irradiated: 77.8%±8.2; recovery: 83.0%±5.7), but a significant difference ($p < 0.05$) was observed only for the recovery condition. A significant difference in mortality ($p < 0.05$) was observed from 72 hpf for both irradiated (89.9%±4.9) and recovery (98.4%±0.7) groups compared to controls (56.1% ± 5.9). No statistical difference was observed between the irradiated and recovery conditions. Control's mortality remained similar until the last day (6 dpf) of the experiment (57.2%±5.7), whereas it reached 100% for the irradiated group and 99.5%±0.5 for the recovery group.

3.2. F1 abnormalities after parental exposure

Malformations (pericardium edema and yolk reserve edema) were observed in F1 72 hpf larvae after parental exposure to IRs (Figure 3A). A significant increase ($p < 0.05$) of yolk reserve area was observed in both conditions, irradiated (n=9, 0.319mm^2 ±

0.007) and recovery (n=12, 0.349mm² ± 0.019), compared to the control group (n=6, 0.244mm² ± 0.014), with no difference between them (Figure 3B). After setting F0 irradiated adult fish in control condition for 6 days, their offspring (Resilience_6d) still showed a significant increase ($p < 0.05$) in yolk reserve area (n=11, 0.400mm² ± 0.020) compared to the control group (n=11, 0.241mm² ± 0.009). On the other hand, after 36 days of setting the adults in control condition, no morphological defects were observed in their offspring (Resilience_36d). For pericardial area, statistical difference ($p < 0.05$) was observed only for resilience_6d compared to control group (Figure 3C).

3.3. Transmitted macro-molecules from F0 to F1

3.3.1. Glucocorticoid regulation in the gonad

Cortisol concentration in F0 female gonads after reproduction was not impacted by IR (Figure 4A). Indeed, its concentration reached 0.036ng.mg^{-1} ± 0.005 for irradiated group (n=6) and 0.041ng.mg^{-1} ± 0.006 for control group (n=6). However, at the transcriptional level (RNAseq), a down-regulation of *nr3c1*, the glucocorticoid receptor, was observed in F0 female gonads (n=8) after irradiation (Figure 4B). Moreover, many genes involved in cortisol biosynthesis were also down-regulated (*cyp11a1, cyp11a2*, *apoa1a*, *apoeb*, *npc2*, *fdx1, fdx1b*).

3.3.2. VTG analysis in eggs

Western-blot analysis, using an anti-VTG antibody on 24 hpf F1 embryos (n=7 per condition), revealed two bands at around 26 and 30 kDa (Figure S3), but not the band corresponding to the whole VTG (around 150 kDa). Whatever the band considered, i.e. total one, 30kDa band intensity or 26 kDa band intensity, or the ratio between intensities, no significant difference was observed between control and irradiated groups (Figure S4). However, the transcription level of the gene encoding for the

enzyme responsible for VTG cleavage, cathepsin D (*ctsd*), was down-regulated (Log2FoldChange= -0.5, FDR <0.01).

3.4. ***Ovarian transcriptome***

Differential gene expression was assessed in pairwise comparison between irradiated and control ovaries (n=8 per condition). The total number of Differentially Expressed Genes (DEG) (FDR < 0.05), up and down regulated genes with a fold change superior to 2 (|log2fold change| ≥ 1 and FDR < 0.05), up regulated genes (log2fold change ≥ 1 and FDR < 0.05) and down regulated genes (log2fold change ≤ 1 and FDR < 0.05) reached 9182, 5348, 3234 and 2114, respectively.

Pathways enrichment analyses were then performed using GO repositories (with zebrafish orthologues) and the KEGG database (with human orthologous genes).

Considering all dysregulated genes (FDR <0.05) or only up regulated or down regulated genes (|log2fold change | ≥ 1 and FDR < 0.05), 304, 394 and 83 GO terms were enriched, respectively (Table S2). The most dysregulated pathways from dysregulated genes were related to ribosomes (GO:0022613, ribonucleoprotein complex biogenesis, p.adjust=1.74E-22) and DNA damage (GO:0006281, DNA repair, p.adjust= 7.25E-11) (Figure 5A). GO terms linked to ribosomes synthesis were principally represented by down regulated genes (GO:0042254, ribosome biogenesis, p.adjust= 5.28E-09). We also found other GO terms associated with DNA damage and genotoxicity that were highly dysregulated (GO:0051403, stress-activated MAPK cascade, p.adjust= 0.02; GO:0097190, apoptotic signalling pathway, p.adjust= 0.02; GO:0006302, double-strand break repair, p.adjust= 2.72E-04). For DNA damage group, transcripts of the p53 pathway were all up-regulated (Figure 5B, *tp53bp1*, *tp53bp2a*, *tp53bp2b*, *deltaNp63*) while other genes involved in DNA repairs were

down-regulated (*gadd45ab*, *rad51*, *xrcc6*, *xrcc5*, *ddb2*, *creb1a*, *creb1b*, *polb*). Transcripts involved in the fight against oxidative stress were also down-regulated (*gpx1a*, *gpx1b*, *gsta.1*, *sod1*, *sod2*).

GO terms linked to reproduction (GO:0022414, reproductive process, p.adjust= 6.21E-04; GO:0048477, oogenesis, p.adjust= 3.12E-04) and germ line production (GO:0007281, germ cell development, p.adjust=0.03) were also impacted by irradiation.

Dysregulated genes involved in oogenesis and ribosomes are presented in Figure 5B. They were mostly down-regulated (*buc*, *rpl, rps*) while *macf1a* was up-regulated.

Among the upregulated genes, many were involved in morphogenesis (GO:0060560, developmental growth involved in morphogenesis, p.adjust= 1.13E-04) and embryo axis establishment (GO:0009952, anterior/posterior pattern specification, p.adjust=0.01; GO:0009953, dorsal ventral pattern formation, p.adjust= 2.73E-03, GO:0016055, Wnt signalling pathway, p.adjust= 9.96E-03). Transcripts related to embryonic development, and in particular in axis development, were mainly up-regulated (Figure 5B, *ctnnb2*, *runx2b, smad* genes), but some important factors for axis establishment were down-regulated (*grip2a*, *sybu*, *pou5f3*, *ndr1*, *gdf3*). Transcripts related to the maternal to zygotic transition (MZT) stage were also up-regulated (*drosha*, *dicer1*, *ago2*, *ago3b*, *ago4*, *ythdf2*).

Considering dysregulated genes (FDR <0.05), or only up regulated genes or down regulated genes 20, 15 and 5 KEGG pathways were enriched, respectively and are presented in Figure 6. KEGG enrichment analysis with only upregulated genes were consistent to GO terms enrichment since pathway linked to embryo development were impacted (dre04068, FoxO signalling pathway, p.adjust= 0.04; dre04330, Notch

signalling pathway, p.adjust= 4.88E-03; dre04340, Hedgehog signalling pathway, p.adjust= 3.53E-03; dre04310, Wnt signalling pathway, p.adjust= 3.90E-04; dre04012, ErbB signalling pathway, p.adjust= 1.56E-05). As previously described, many dysregulated genes or down regulated genes were involved in oogenesis (dre04914, Progesterone mediated oocyte maturation, p.adjust= 4.23E-03; dre04114, Oocyte meiosis, p.adjust= 4.23E-03) and ribosomes (dre03008, Ribosome biogenesis in eukaryotes, p.ajust= 3.61E-06).

4. Discussion

In order to investigate the molecular cascade that induce drastic effects on offspring, a high dose rate of 50 $mGy.h^{-1}$ was purposely chosen. Here we detected significant differences on offspring survival rates at 72 hpf (Figure 2). Moreover, malformations, mainly yolk reserve edema, were observed for irradiated, recovery and resilience_6d conditions after parental irradiation (Figure 3). Offspring effects were therefore observed even when only genitors were irradiated. Moreover, Resilience_6d condition show altered offspring, while genitors were in control condition. This supports that deleterious effects in genitors induce non-viable offspring. Several maternal factors being transmitted to embryo could explain these phenotypes. This is why this study initially focused on maternal involvement. Paternal involvement cannot be totally excluded but seems less obvious to us in the present case where effects are very early, probably before zygote genome activation.

4.1. IR altered maternal provided molecules

4.1.1. IR led to oxidative stress and DNA damages in ovary

The RNAseq analysis on female gonads showed an evidence of DNA damage, confirming previous results using COMET assay (Guirandy et al., 2019; Hurem et al.,

2018). Enrichment analysis on GO terms (Figure 5A) revealed typical biological processes related to DNA damage and oxidative stress (« stress-activated MAPK cascade »). Enrichment analysis on KEGG pathways (Figure 6) showed IR-induced effects on « FoxO signalling pathway » and « ErbB signalling pathway », which are involved in oxidative stress and cancer development, respectively, and already known to be impacted by radiations (Dent et al., 2003; Luo et al., 2007).

Several genes involved in apoptosis via the P53 pathway (*tp53bp1*, *tp53bp2*, *deltaNp63*) (Elersek et al., 2022)) were up-regulated (Figure 5B). p53 genes, required for radiation-induced apoptosis in mouse (Lowe et al., 1993), are involved in cell cycle arrest but also in damage repair in zebrafish (Canedo and Rocha, 2021; Sandrini et al., 2009). However, several genes involved in DNA repair mechanisms, mainly in double strand break reparation (Canedo and Rocha, 2021; Reinardy et al., 2013; Sandrini et al., 2009) were also down regulated (Figure 5B, *gadd45ab*, *rad51*, *xrcc6*, *xrcc5*, *ddb2*, *creb1a*, *creb1b*, *polb*). In addition, genes involved in the fight against oxidative stress (Figure 5B, *gpx1a*, *gpx1b*, *gsta.1*, *sod1*, *sod2*) were down regulated, suggesting an alteration of the antioxidant response and ROS imbalance. The altered oxidative balance in genitors did not seem to disturb the reproductive performances of adults but could contribute to adverse effects on oocyte DNA, as explain before, or on offspring development, as proposed by W. Huang et al. 2020. Thus, a direct effect of ROS or an induced effect on the integrity of the maternal DNA in oocytes could occur, thereby producing a future non-viable offspring. However, fertilization and first stages of embryo development (gastrulation) seemed to occur normally.

4.1.2. IR did not impact cortisol and VTG

Maternal cortisol is necessary for proper embryo development (Colson et al., 2015; Faught and Vijayan, 2018). Altered maternal concentration of cortisol may yield cardiac

oedema as described by Nesan and Vijayan, 2012. In our study, even if cardiac oedema were observed in offspring at 72 hpf for resilience-6d (Figure 3E), no effect was observed in ovarian cortisol level (Figure 4A). However, maternal glucocorticoid receptor transcripts (*nr3c1 or gr*), that participate in the maternal programming of embryo development (Pikulkaew et al. 2011), were down regulated in female gonads (Figure 4B). Furthermore, other transcripts involved in cortisol biosynthetic process were also differentially regulated (Figure 4B, *cyp11a1*, *cyp11a2*, *apoa1a*, *apoeb*, *npc2*, *fdx1*, *fdx1b*) (Facchinello et al., 2017; Nesan and Vijayan, 2012). Thus, even if these molecular effects were not associated with changes at the metabolite level, an effect of cortisol could not be totally discarded.

Moreover, yolk reserve oedemas (Figure 3) were observed in offspring at 72 hpf for irradiated, recovery and resilience-6d, suggesting a nutrient reserve disruption (observed for many pollutants in fish). The gene encoding for the enzyme responsible for VTG cleavage, cathepsin D (*ctsd*), was down regulated, suggesting less VTG conversion into storage forms that are required for early development (Yilmaz et al., 2018). However, the total quantity of vitellogenin products that can bind to the antibody was not impacted by irradiation, and yolk reserve areas were higher after irradiation suggesting rather a non-consumption of reserves in larvae from irradiated parents. Since maternally-provided *ctsd* transcripts allows proper treatment and consumption of yolk proteins by embryos (Follo et al., 2011), down-regulation of this gene could explain the non-consumption. Cortisol and VTG were non-impacted by IRs and cannot explain mortality and malformation. Molecular alteration on cortisol biosynthesis and VTG degradation encourage us to further investigations.

Another hypothesis to identify mechanisms of transmitted effects was that altered maternal transcriptome, after irradiation exposure, could have early and delayed consequences on embryo development.

4.2. IR altered oocyte development

Enrichment analysis showed GO terms and KEGG pathways linked to reproduction and oogenesis, including « oocyte meiosis » and «oocyte development » (Figure 5A, Figure 6). Embryo development success is dependent on mRNA, molecules, germplasm and organelles (golgi and mitochondria) aggregated in the Balbiani body (Bb) during maternal oogenesis (Jamieson-Lucy and Mullins, 2019; Marlow, 2010). Three maternal genes are involved in Bb development (Marlow, 2010). Among them, *bucky ball* (*buc*), that is necessary to establish the polarity of the egg (animal-vegetal axis), was down regulated after irradiation (Figure 5B) (Marlow, 2010). Maternal *buc* deficiency is known to induce polyspermy with normal cell division after fertilization and ultimately embryo death (Jamieson-Lucy and Mullins, 2019). This could explain death at around 72 hpf here and at around 24 hpf in the study of Guirandy et al., 2019. Microtubule actin crosslinking factor 1 (*macf1*) is critical for Bb disassembly ensuring the dispersion of mRNA along the animal-vegetal axis (Jamieson-Lucy and Mullins, 2019). In our study, *macf1a* was up-regulated (Figure 5B), potentially leading to disturbed mRNA distribution and finally to embryo death.

Oogenesis also allows the accumulation of maternal ribosomal proteins (RP) in order to support early embryo development until zygotic genome activation (ZGA) (Mercer et al., 2021). Precise control of ribosome biogenesis is vital for cell survival (Danilova et al., 2008) and therefore for preventing abnormalities during zebrafish embryonic development. For example, a deficiency in *rpl11* induces an increase in yolk reserve size in mutants, reflecting a slow metabolism, and a decrease in larvae size (Palasin

et al., 2019). These two phenotypes were also observed in this study and by Guirandy et al. 2019. Enrichment analysis (Figure 5A, Figure 6) highlighted different processes linked to ribosome synthesis (« ribonucleoprotein complex biogenesis », « ribosome biogenesis », « Ribosome biogenesis in eukaryotes »). Several RP transcripts that were down-regulated (Figure 5B, *rpl10a, rpl11*, *rpl23*) are known to activate the p53 pathway (as observed in 4.1.1) (Chakraborty et al., 2009; Palasin et al., 2019). Down-regulation of *rps19*, *rps8a, rps8b, rps11* and *rps18* were associated with an up-regulation of deltaNp63, as previously observed (Danilova et al., 2008). RP deficiency via its impact on cell division and on the p53 pathway, could represent a further explanation for the observed early effects on offspring after maternal gamma irradiation.

It is clear that irradiation altered proper oocyte development. Thus, it could produce defective offspring. Next, we wondered if altered maternal mRNAs could induce later, i.e; after spawning and fertilization, effects in addition to direct impacts on oocytes.

4.3. IR altered maternal mRNAs needed for offspring development

4.3.1. Embryo axis establishment

Other maternal mRNAs needed for embryo development were also impacted by irradiation. Among them, many are accumulated in Bb and are involved in embryo axis establishment (Marlow, 2010). Enrichment analysis revealed GO terms and KEGG pathways involved in embryo development (Figure 5A, Figure 6), in particular with genes that were up-regulated. Several biological processes concerning the morphogenesis were impacted (“cell projection morphogenesis”, “embryonic organ morphogenesis”, “dorsal/ventral pattern formation”,”Wnt signalling pathway”). Since

oocyte polarity and maternal mRNAs were impacted (4.2), it appears not aberrant that maternal mRNAs governing embryo axis establishment were also disturbed.

Maternal β-catenin and *grip2a* are the first indication of dorso-ventral polarity (Langdon and Mullins, 2011). β-catenin genes (*ctnnb1* and *ctnnb2*) were down-regulated and up-regulated, respectively (Figure 5B). *ctnnb1* is known to act upstream at the molecular level and *ctnnb2* then acts on the physical establishment of the axis. Opposite regulations for these two key stages could alter proper embryo development (Zhang et al., 2012). For example, up-regulation of β-catenin leads to hyper-dorsalization (Kelly et al., 1995; Nojima et al., 2004; Sumoy et al., 1999). *grip2a* that acts upstream or in parallel to maternal β-catenin was down-regulated (Figure 5B). In the same way, *syntabulin* (*sybu*) was down regulated (Figure 5B) and loss of maternal *sybu* was found to induce ventralization and failure to activate the Wnt signalling pathway, which is required to initiate dorsal cell fate specification (Langdon and Mullins, 2011).

In contrast, the Bone Morphogenetic Protein signalling pathway, involved in ventral axis specification, was not impacted. However, an initiator gene of this pathway, *pou5f3* (Abrams and Mullins, 2009; Flores et al., 2008; “Maternal Effect Genes in Development, Volume 140 - 1st Edition,” n.d.) was down-regulated (Figure 5B). Moreover, several ventral genes were also dysregulated (Figure 5B, *runx2b*, smad1, *smad2*, *smad4a*, *smad5*, *smad6a*) (Pelegri, 2003). As for dorsal axis specification, genes involved in ventral axis specification seemed to be highly dysregulated that could lead to the observed malformations and non-viable embryos.

Finally, the left/right axis, needed to organ asymmetry such as brain and heart, is mainly governed by the nodal signalling pathway (Bisgrove et al., 2017; Miccoli et al., 2017), which was not impacted. However, a key gene of this pathway, *ndr1* was down-

511 regulated (Figure 5B). This was not surprising since its positive co-factor, *gdf3*
512 (Bisgrove et al., 2017), was also down-regulated. *Gdf3* mutation leads to embryo
513 death. Gamma irradiation thus impacted maternal transcripts necessary to asymmetry
514 development and could explain observed mortality.

515 *4.3.2. Maternal mRNA degradation*

516 Failure of maternal mRNA degradation concomitantly to zygotic genome activation
517 (ZGA) can lead to miscoordinated gene expression (Chang et al., 2018; Walser and
518 Lipshitz, 2011). The best-known degradation mechanism is deadenylation. The
519 majority of maternal transcripts are therefore deadenylated and degraded between 4
520 and 6 hpf (Chang et al., 2018; Walser and Lipshitz, 2011) at the same time as ZGA.
521 Interestingly, enrichment analysis showed an impact on the biological process "positive
522 regulation of nuclear-transcribed mRNA catabolic process, deadenylation-dependent
523 decay" (Figure 5), which could reflect a deregulation of maternal mRNA catabolic
524 process after irradiation. We also detected the dysregulation of many factors involved
525 in the maturation of miRNA (*drosha, dicer1, ago2, ago3b, ago4*) as mentioned after
526 parental irradiation in Martín et al., 2021. As MiR-430 facilitates the deadenylation of
527 maternal mRNAs (Giraldez et al., 2006; Laue et al., 2019; Liu et al., 2020; Yao et al.,
528 2014), it is possible that deregulation of miRNA production contribute to the increased
529 in embryonic mortality . Another degradation way during maternal to zygotic transition
530 stage is uridylation, done by *tut7* which was down regulated (Figure 5B) (Chang et al.,
531 2018). Furthermore, *igf2bp3,* a gene encoding for a protein involved in maternal mRNA
532 stability (Ren et al., 2020), was up-regulated (Figure 5B). whereas *ythdf2*, involved in
533 maternal transcript degradation, was down-regulated (Figure 5B) (Ren et al., 2020).
534 These results suggest a disturbed mRNA degradation process in female gonads.
535 Maternal mRNA could thus be rapidly degraded and could not support early

development or could alter the temporal pattern of gene expression during early development.

5. Conclusions

This paper highlighted transmitted effect from genitors to offspring after 10 days of gamma irradiation at 50 mGy.h-1. No phenotypic effect was observed in genitors, notably on reproductive performances (reproductive success and fecundity). Early mortality in offspring in link to parental transmitted effects was observed as no difference was observed between irradiated and recovery conditions. Moreover, early malformations were observed in offspring after parental irradiation. The main objective was to get mechanistic insights into the impacts of irradiation at the cellular and molecular levels in order to identify mechanisms behind phenotypic effects on offspring.

Cortisol level in F0 female gonads after reproduction was not impacted by irradiation. However, it should be necessary to measure cortisol in embryos to refute its involvement in F1 mortality. Despite a down-regulation of cathepsin D in maternal gonads, VTG analysis in embryos did not highlight any different amount nor distribution of maturation products which suggests no nutrition defect for embryos. This non-effect should be however confirmed by measuring the whole VTG protein. Oogenesis and maternal factors (mRNA) required for production of viable offspring and their development were significantly altered, supporting maternal transmission of IR-induced effects.

This first multigenerational approach to link phenotype to molecular events highlighted an important effect of female irradiation on offspring viability with (i) an impact of irradiation on oocyte development and (ii) an impact on maternal mRNAs needed later

for embryonic development. However, paternal contribution should not be excluded and should be investigated in future experiments, since they were also exposed. Further experiments would be to perform a cross-exposure (only female exposed) to assess maternal role. Finally, offspring transcriptomic analysis before and after the maternal-to-zygotic transition should be interesting to define more precisely the role of maternal mRNAs. Our data could be used to improve the Adverse Outcome Pathways and challenge the environmental risk assessment method currently deployed.

Funding sources

Funding: This work was supported by the Institut de Radioprotection et de Sûreté Nucléaire (IRSN).

References

Abrams, E.W., Mullins, M.C., 2009. Early zebrafish development: It's in the maternal genes. Curr. Opin. Genet. Dev. 19, 396–403. https://doi.org/10.1016/j.gde.2009.06.002

Beresford, N.A., Horemans, N., Copplestone, D., Raines, K.E., Orizaola, G., Wood, M.D., Laanen, P., Whitehead, H.C., Burrows, J.E., Tinsley, M.C., Smith, J.T., Bonzom, J.-M., Gagnaire, B., Adam-Guillermin, C., Gashchak, S., Jha, A.N., de Menezes, A., Willey, N., Spurgeon, D., 2020. Towards solving a scientific controversy – The effects of ionising radiation on the environment. J. Environ. Radioact. 211, 106033. https://doi.org/10.1016/j.jenvrad.2019.106033

Bisgrove, B., Su, Y.-C., Yost, H., 2017. Maternal Gdf3 is an obligatory cofactor in Nodal signaling for embryonic axis formation in zebrafish. eLife. https://doi.org/10.7554/eLife.28534

Canedo, A., Rocha, T.L., 2021. Zebrafish (Danio rerio) using as model for genotoxicity and DNA repair assessments: Historical review, current status and trends. Sci. Total Environ. 762, 144084. https://doi.org/10.1016/j.scitotenv.2020.144084

Car, C., Gilles, A., Armant, O., Burraco, P., Beaugelin-Seiller, K., Gashchak, S., Camilleri, V., Cavalié, I., Laloi, P., Adam-Guillermin, C., Orizaola, G., Bonzom, J.-M., 2022. Unusual evolution of tree frog populations in the Chernobyl exclusion zone. Evol. Appl. 15, 203–219. https://doi.org/10.1111/eva.13282

Chakraborty, A., Uechi, T., Higa, S., Torihara, H., Kenmochi, N., 2009. Loss of Ribosomal Protein L11 Affects Zebrafish Embryonic Development through a p53-Dependent Apoptotic Response. PLOS ONE 4, e4152. https://doi.org/10.1371/journal.pone.0004152

Chang, H., Yeo, J., Kim, J.-G., Kim, H., Lim, J., Lee, M., Kim, H.H., Ohk, J., Jeon, H.-Y., Lee, H., Jung, H., Kim, K.-W., Kim, V.N., 2018. Terminal Uridylyltransferases Execute Programmed Clearance of Maternal Transcriptome in Vertebrate Embryos. Mol. Cell 70, 72-82.e7. https://doi.org/10.1016/j.molcel.2018.03.004

595 Chen, M.-F., Huang, C.-Z., Pu, D.-Y., Zheng, C.-Y., Yuan, K.-M., Jin, X.-X., Zhang, Y.-G., Jin, L., 2015.
596 Toxic effects of CdSe/ZnS QDs to zebrafish embryos. Huanjing KexueEnvironmental Sci. 36,
597 719–726. https://doi.org/10.13227/j.hjkx.2015.02.046
598 Colson, V., Valotaire, C., Geffroy, B., Kiilerich, P., 2015. Egg Cortisol Exposure Enhances Fearfulness in
599 Larvae and Juvenile Rainbow Trout. Ethology 121, 1191–1201.
600 https://doi.org/10.1111/eth.12437
601 Cunningham, K., Hinton, T.G., Luxton, J.J., Bordman, A., Okuda, K., Taylor, L.E., Hayes, J., Gerke, H.C.,
602 Chinn, S.M., Anderson, D., Laudenslager, M.L., Takase, T., Nemoto, Y., Ishiniwa, H., Beasley,
603 J.C., Bailey, S.M., 2021. Evaluation of DNA damage and stress in wildlife chronically exposed
604 to low-dose, low-dose rate radiation from the Fukushima Dai-ichi Nuclear Power Plant
605 accident. Environ. Int. 155, 106675. https://doi.org/10.1016/j.envint.2021.106675
606 Danilova, N., Sakamoto, K.M., Lin, S., 2008. Ribosomal protein S19 deficiency in zebrafish leads to
607 developmental abnormalities and defective erythropoiesis through activation of p53 protein
608 family. Blood 112, 5228–5237. https://doi.org/10.1182/blood-2008-01-132290
609 Dent, P., Yacoub, A., Contessa, J., Caron, R., Amorino, G., Valerie, K., Hagan, M.P., Grant, S., Schmidt-
610 Ullrich, R., 2003. Stress and Radiation-Induced Activation of Multiple Intracellular Signaling
611 Pathways1. Radiat. Res. 159, 283–300. https://doi.org/10.1667/0033-
612 7587(2003)159[0283:SARIAO]2.0.CO;2
613 Eaton, S.L., Roche, S.L., Hurtado, M.L., Oldknow, K.J., Farquharson, C., Gillingwater, T.H., Wishart,
614 T.M., 2013. Total Protein Analysis as a Reliable Loading Control for Quantitative Fluorescent
615 Western Blotting. PLOS ONE 8, e72457. https://doi.org/10.1371/journal.pone.0072457
616 Facchinello, N., Skobo, T., Meneghetti, G., Colletti, E., Dinarello, A., Tiso, N., Costa, R., Gioacchini, G.,
617 Carnevali, O., Argenton, F., Colombo, L., Dalla Valle, L., 2017. Nr3c1 null mutant zebrafish are
618 viable and reveal DNA-binding-independent activities of the glucocorticoid receptor. Sci. Rep.
619 7. https://doi.org/10.1038/s41598-017-04535-6
620 Faught, E., Vijayan, M., 2018. Maternal stress and fish reproduction: The role of cortisol revisited.
621 Fish Fish. https://doi.org/10.1111/FAF.12309
622 Finn, R.N., 2007. Vertebrate Yolk Complexes and the Functional Implications of Phosvitins and Other
623 Subdomains in Vitellogenins1. Biol. Reprod. 76, 926–935.
624 https://doi.org/10.1095/biolreprod.106.059766
625 Flores, M.V.C., Lam, E.Y.N., Crosier, K.E., Crosier, P.S., 2008. Osteogenic transcription factor Runx2 is
626 a maternal determinant of dorsoventral patterning in zebrafish. Nat. Cell Biol. 10, 346–352.
627 https://doi.org/10.1038/ncb1697
628 Follo, C., Ozzano, M., Mugoni, V., Castino, R., Santoro, M., Isidoro, C., 2011. Knock-Down of Cathepsin
629 D Affects the Retinal Pigment Epithelium, Impairs Swim-Bladder Ontogenesis and Causes
630 Premature Death in Zebrafish. PLOS ONE 6, e21908.
631 https://doi.org/10.1371/journal.pone.0021908
632 Geras'kin, S.A., Fesenko, S.V., Volkova, P.Yu., Isamov, N.N., 2021. What Have We Learned about the
633 Biological Effects of Radiation from the 35 Years of Analysis of the Consequences of the
634 Chernobyl NPP Accident? Biol. Bull. 48, 2105–2126.
635 https://doi.org/10.1134/S1062359021120050
636 Giraldez, A.J., Mishima, Y., Rihel, J., Grocock, R.J., Van Dongen, S., Inoue, K., Enright, A.J., Schier, A.F.,
637 2006. Zebrafish MiR-430 promotes deadenylation and clearance of maternal mRNAs. Science
638 312, 75–79. https://doi.org/10.1126/science.1122689
639 Guirandy, N., Gagnaire, B., Camilleri, V., Cavalié, I., Pierron, F., Gonzalez, P., Simon, O., 2022.
640 Multigenerational exposure to gamma radiation affects offspring differently over generations
641 in zebrafish. Aquat. Toxicol. 244, 106101. https://doi.org/10.1016/j.aquatox.2022.106101
642 Guirandy, N., Gagnaire, B., Frelon, S., Munch, T., Dubourg, N., Camilleri, V., Cavalié, I., Floriani, M.,
643 Arcanjo, C., Houdigui, S.M.E., Armant, O., Adam-Guillermin, C., Gonzalez, P., Simon, O., 2019.
644 Adverse effects induced by chronic gamma irradiation in progeny of adult fish not affecting
645 parental reproductive performance. Environ. Toxicol. Chem. 38, 2556–2567.
646 https://doi.org/10.1002/etc.4562

Huang, W., Zheng, S., Wang, X., Cai, Z., Xiao, J., Liu, C., Wu, K., 2020. A transcriptomics-based analysis of toxicity mechanisms of zebrafish embryos and larvae following parental Bisphenol A exposure. Ecotoxicol. Environ. Saf. 205. https://doi.org/10.1016/j.ecoenv.2020.111165

Hurem, S., Gomes, T., Brede, D.A., Lindbo Hansen, E., Mutoloki, S., Fernandez, C., Mothersill, C., Salbu, B., Kassaye, Y.A., Olsen, A.-K., Oughton, D., Aleström, P., Lyche, J.L., 2017. Parental gamma irradiation induces reprotoxic effects accompanied by genomic instability in zebrafish (Danio rerio) embryos. Environ. Res. 159, 564–578. https://doi.org/10.1016/j.envres.2017.07.053

Hurem, S., Gomes, T., Brede, D.A., Mayer, I., Lobert, V.H., Mutoloki, S., Gutzkow, K.B., Teien, H.-C., Oughton, D., Aleström, P., Lyche, J.L., 2018. Gamma irradiation during gametogenesis in young adult zebrafish causes persistent genotoxicity and adverse reproductive effects. Ecotoxicol. Environ. Saf. 154, 19–26. https://doi.org/10.1016/j.ecoenv.2018.02.031

Jamieson-Lucy, A., Mullins, M.C., 2019. Chapter One - The vertebrate Balbiani body, germ plasm, and oocyte polarity, in: Lehmann, R. (Ed.), Current Topics in Developmental Biology, The Immortal Germline. Academic Press, pp. 1–34. https://doi.org/10.1016/bs.ctdb.2019.04.003

Kelly, G.M., Erezyilmaz, D.F., Moon, R.T., 1995. Induction of a secondary embryonic axis in zebrafish occurs following the overexpression of β-catenin. Mech. Dev. 53, 261–273. https://doi.org/10.1016/0925-4773(95)00442-4

Langdon, Y.G., Mullins, M.C., 2011. Maternal and zygotic control of zebrafish dorsoventral axial patterning. Annu. Rev. Genet. 45, 357–377. https://doi.org/10.1146/annurev-genet-110410-132517

Laue, K., Rajshekar, S., Courtney, A.J., Lewis, Z.A., Goll, M.G., 2019. The maternal to zygotic transition regulates genome-wide heterochromatin establishment in the zebrafish embryo. Nat. Commun. 10, 1551. https://doi.org/10.1038/s41467-019-09582-3

Liu, Y., Zhu, Z., Ho, I.H.T., Shi, Y., Li, J., Wang, X., Chan, M.T.V., Cheng, C.H.K., 2020. Genetic Deletion of miR-430 Disrupts Maternal-Zygotic Transition and Embryonic Body Plan. Front. Genet. 11. https://doi.org/10.3389/fgene.2020.00853

Lowe, S.W., Ruley, H.E., Jacks, T., Housman, D.E., 1993. p53-dependent apoptosis modulates the cytotoxicity of anticancer agents. Cell 74, 957–967. https://doi.org/10.1016/0092-8674(93)90719-7

Luo, X., Puig, O., Hyun, J., Bohmann, D., Jasper, H., 2007. Foxo and Fos regulate the decision between cell death and survival in response to UV irradiation. EMBO J. 26, 380–390. https://doi.org/10.1038/sj.emboj.7601484

Marlow, F.L., 2010. Oocyte Polarity and the Embryonic Axes: The Balbiani Body, an Ancient Oocyte Asymmetry, Maternal Control of Development in Vertebrates: My Mother Made Me Do It! Morgan & Claypool Life Sciences.

Martín, L., Kamstra, J.H., Hurem, S., Lindeman, L.C., Brede, D.A., Aanes, H., Babiak, I., Arenal, A., Oughton, D., Salbu, B., Lyche, J.L., Aleström, P., 2021. Altered non-coding RNA expression profile in F1 progeny 1 year after parental irradiation is linked to adverse effects in zebrafish. Sci. Rep. 11, 4142. https://doi.org/10.1038/s41598-021-83345-3

Maternal Effect Genes in Development, Volume 140 - 1st Edition [WWW Document], n.d. URL https://www.elsevier.com/books/maternal-effect-genes-in-development/marlow/978-0-12-815220-1 (accessed 2.9.22).

McCormick, M.I., 1999. Experimental test of the effect of maternal hormones on larval quality of a coral reef fish. Oecologia 118, 412–422. https://doi.org/10.1007/s004420050743

Mercer, M., Jang, S., Ni, C., Buszczak, M., 2021. The Dynamic Regulation of mRNA Translation and Ribosome Biogenesis During Germ Cell Development and Reproductive Aging. Front. Cell Dev. Biol. 9. https://doi.org/10.3389/fcell.2021.710186

Miccoli, A., Dalla Valle, L., Carnevali, O., 2017. The maternal control in the embryonic development of zebrafish. Gen. Comp. Endocrinol. 245, 55–68. https://doi.org/10.1016/j.ygcen.2016.03.028

Moritz, C.P., 2017. Tubulin or Not Tubulin: Heading Toward Total Protein Staining as Loading Control in Western Blots. PROTEOMICS 17, 1600189. https://doi.org/10.1002/pmic.201600189

699 Murat El Houdigui, S., Adam-Guillermin, C., Loro, G., Arcanjo, C., Frelon, S., Floriani, M., Dubourg, N.,
700 Baudelet, E., Audebert, S., Camoin, L., Armant, O., 2019. A systems biology approach reveals
701 neuronal and muscle developmental defects after chronic exposure to ionising radiation in
702 zebrafish. Sci. Rep. 9, 20241. https://doi.org/10.1038/s41598-019-56590-w
703 Nesan, D., Vijayan, M.M., 2016. Maternal Cortisol Mediates Hypothalamus-Pituitary-Interrenal Axis
704 Development in Zebrafish. Sci. Rep. 6, 22582. https://doi.org/10.1038/srep22582
705 Nesan, D., Vijayan, M.M., 2012. Embryo exposure to elevated cortisol level leads to cardiac
706 performance dysfunction in zebrafish. Mol. Cell. Endocrinol. 363, 85–91.
707 https://doi.org/10.1016/j.mce.2012.07.010
708 Nojima, H., Shimizu, T., Kim, C.-H., Yabe, T., Bae, Y.-K., Muraoka, O., Hirata, T., Chitnis, A., Hirano, T.,
709 Hibi, M., 2004. Genetic evidence for involvement of maternally derived Wnt canonical
710 signaling in dorsal determination in zebrafish. Mech. Dev. 121, 371–386.
711 https://doi.org/10.1016/j.mod.2004.02.003
712 Palasin, K., Uechi, T., Yoshihama, M., Srisowanna, N., Choijookhuu, N., Hishikawa, Y., Kenmochi, N.,
713 Chotigeat, W., 2019. Abnormal development of zebrafish after knockout and knockdown of
714 ribosomal protein L10a. Sci. Rep. 9, 18130. https://doi.org/10.1038/s41598-019-54544-w
715 Pelegri, F., 2003. Maternal factors in zebrafish development. Dev. Dyn. Off. Publ. Am. Assoc. Anat.
716 228, 535–554. https://doi.org/10.1002/dvdy.10390
717 Pikulkaew, S., Benato, F., Celeghin, A., Zucal, C., Skobo, T., Colombo, L., Dalla Valle, L., 2011. The
718 knockdown of maternal glucocorticoid receptor mRNA alters embryo development in
719 zebrafish. Dev. Dyn. 240, 874–889. https://doi.org/10.1002/dvdy.22586
720 R Core Team, R.C.T., 2021. R: A language and environment for statistical ## computing. R
721 Foundation for Statistical Computing, Vienna, Austria. [WWW Document]. URL URL
722 https://www.R-project.org/
723 Reinardy, H.C., Syrett, J.R., Jeffree, R.A., Henry, T.B., Jha, A.N., 2013. Cobalt-induced genotoxicity in
724 male zebrafish (Danio rerio), with implications for reproduction and expression of DNA repair
725 genes. Aquat. Toxicol. 126, 224–230. https://doi.org/10.1016/j.aquatox.2012.11.007
726 Ren, F., Lin, Q., Gong, G., Du, X., Dan, H., Qin, W., Miao, R., Xiong, Y., Xiao, R., Li, X., Gui, J.-F., Mei, J.,
727 2020. Igf2bp3 maintains maternal RNA stability and ensures early embryo development in
728 zebrafish. Commun. Biol. 3, 94. https://doi.org/10.1038/s42003-020-0827-2
729 Richon, V.M., Sandhoff, T.W., Rifkind, R.A., Marks, P.A., 2000. Histone deacetylase inhibitor
730 selectively induces p21WAF1 expression and gene-associated histone acetylation. Proc. Natl.
731 Acad. Sci. 97, 10014–10019. https://doi.org/10.1073/pnas.180316197
732 Sadoul, B., Geffroy, B., 2019. Measuring cortisol, the major stress hormone in fishes. J. Fish Biol. 94,
733 540–555. https://doi.org/10.1111/jfb.13904
734 Sandrini, J.Z., Trindade, G.S., Nery, L.E.M., Marins, L.F., 2009. Time-course Expression of DNA Repair-
735 related Genes in Hepatocytes of Zebrafish (Danio rerio) After UV-B Exposure. Photochem.
736 Photobiol. 85, 220–226. https://doi.org/10.1111/j.1751-1097.2008.00422.x
737 Simon, O., Massarin, S., Coppin, F., Hinton, T.G., Gilbin, R., 2011. Investigating the embryo/larval toxic
738 and genotoxic effects of γ irradiation on zebrafish eggs. J. Environ. Radioact. 102, 1039–1044.
739 https://doi.org/10.1016/j.jenvrad.2011.06.004
740 Soares, J., Coimbra, A.M., Reis-Henriques, M.A., Monteiro, N.M., Vieira, M.N., Oliveira, J.M.A.,
741 Guedes-Dias, P., Fontaínhas-Fernandes, A., Parra, S.S., Carvalho, A.P., Castro, L.F.C., Santos,
742 M.M., 2009. Disruption of zebrafish (Danio rerio) embryonic development after full life-cycle
743 parental exposure to low levels of ethinylestradiol. Aquat. Toxicol. 95, 330–338.
744 https://doi.org/10.1016/j.aquatox.2009.07.021
745 Sumoy, L., Kiefer, J., Kimelman, D., 1999. Conservation of intracellular Wnt signaling components in
746 dorsal-ventral axis formation in zebrafish. Dev. Genes Evol. 209, 48–58.
747 https://doi.org/10.1007/s004270050226
748 Vuori, K.A., Kanerva, M., Ikonen, E., Nikinmaa, M., 2008. Oxidative stress during baltic salmon feeding
749 migration may be associated with yolk-sac fry mortality. Environ. Sci. Technol. 42, 2668–
750 2673. https://doi.org/10.1021/es702632c

751 Walser, C.B., Lipshitz, H.D., 2011. Transcript clearance during the maternal-to-zygotic transition. Curr.
752 Opin. Genet. Dev., Differentiation and gene regulation 21, 431–443.
753 https://doi.org/10.1016/j.gde.2011.03.003
754 Yao, Y., Ma, L., Jia, Q., Deng, W., Liu, Z., Zhang, Y., Ren, J., Xue, Y., Jia, H., Yang, Q., 2014. Systematic
755 characterization of small RNAome during zebrafish early developmental stages. BMC
756 Genomics 15, 117. https://doi.org/10.1186/1471-2164-15-117
757 Yilmaz, O., Patinote, A., Nguyen, T., Bobe, J., 2018. Multiple vitellogenins in zebrafish (Danio rerio):
758 quantitative inventory of genes, transcripts and proteins, and relation to egg quality. Fish
759 Physiol. Biochem. 44, 1509–1525. https://doi.org/10.1007/s10695-018-0524-y
760 Zhang, M., Zhang, J., Lin, S.-C., Meng, A., 2012. β-Catenin 1 and β-catenin 2 play similar and distinct
761 roles in left-right asymmetric development of zebrafish embryos. Development 139, 2009–
762 2019. https://doi.org/10.1242/dev.074435

763

764

765

766

767

768

769

770

771

772

773

774

775

776

777

778

779

780

781

782

783

Figures

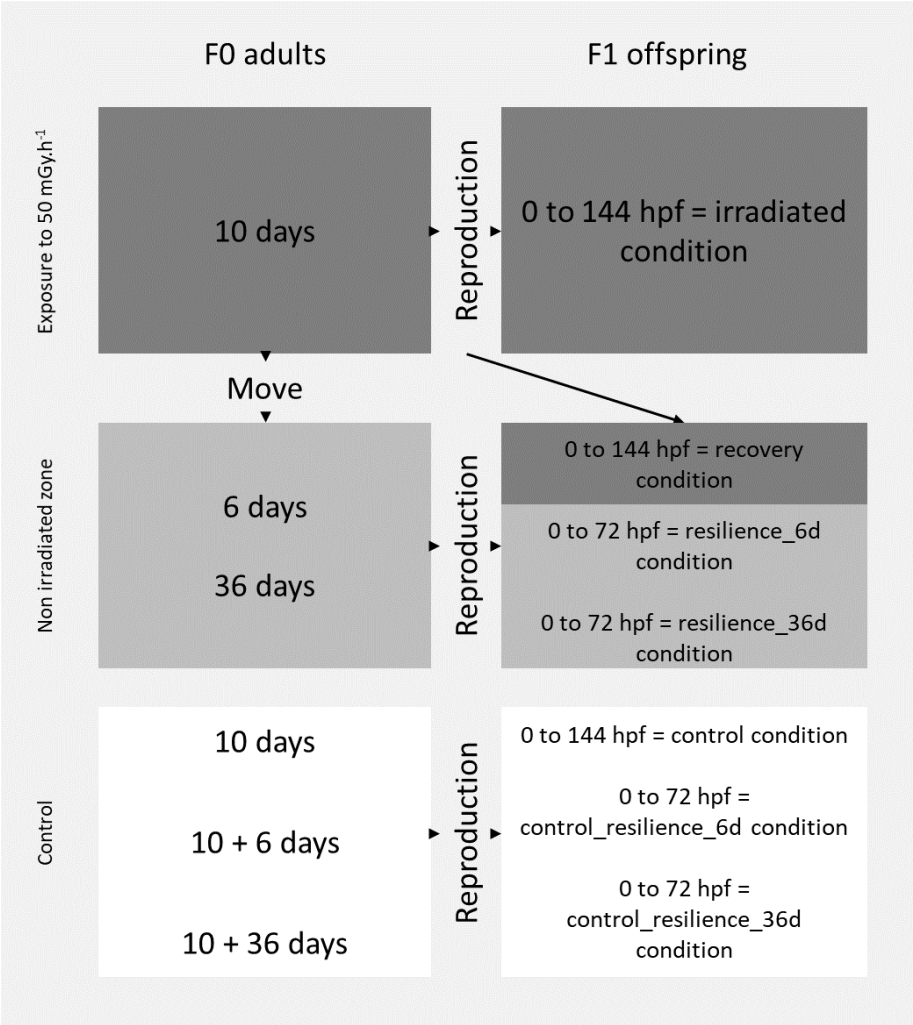

Figure 1: Experimental design and exposure conditions (duration and dose rate (mGy.h^{-1}). F0 adults (24 per conditions) were exposed over 10 days until reproduction. F1 progenies (30 eggs X 6 spawns) were then placed in irradiated (irradiated condition) and non-irradiated (recovery condition) exposure conditions over 6 days. F0 adults were then moved to non-irradiated condition for 6 and 36 days before reproduction. F1 progenies from 6 days F0 (resilience_6d condition) and from 36 days F0 (resilience_36d condition) were then placed in control condition.

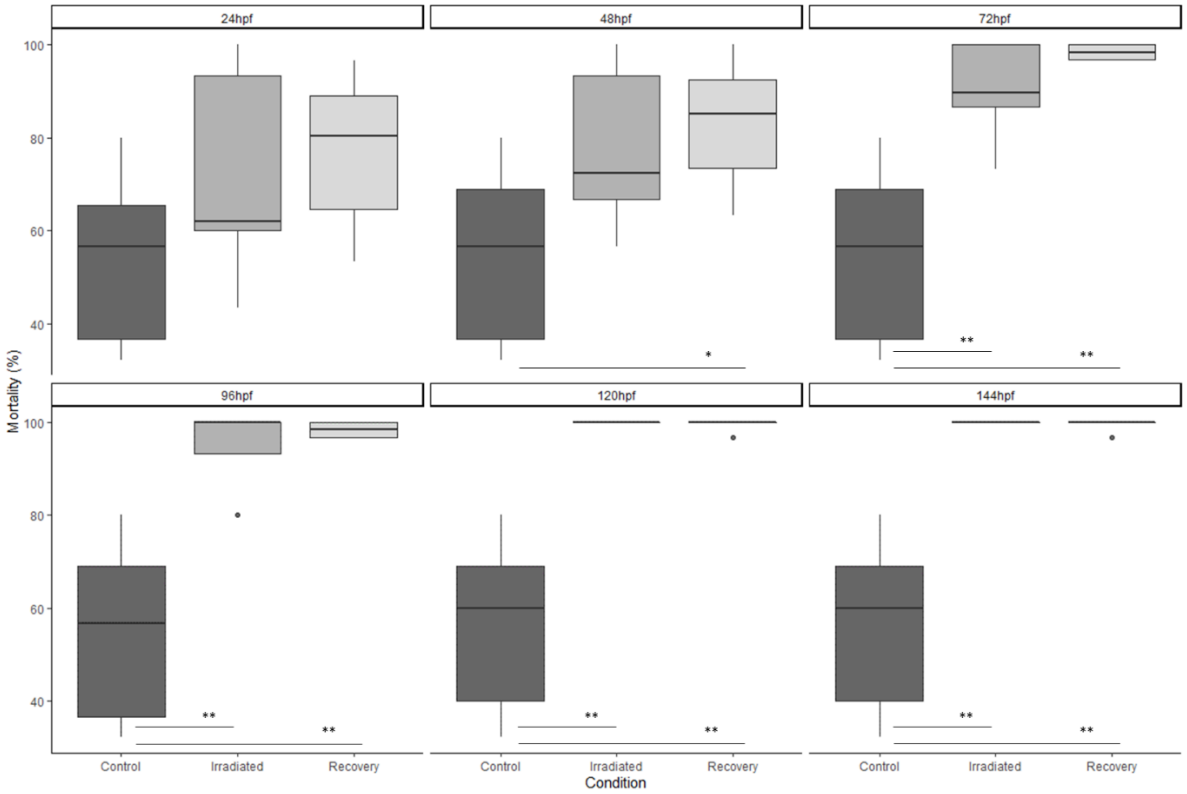

Figure 2: Box-plot of cumulative mortality rates of F1 *(%)) at 24, 48, 72, 96, 120, 144 hpf after control, dose rate exposure to 50 mGy.h^{-1} (irradiated) and recovery conditions. The boxplot represents the 25th and the 75th percentile with the median indicated by the horizontal black line. For control, irradiated and recovery, n=9, n=5, n=6, respectively. * (p < 0.05), ** (p < 0.01), *** (p < 0.001).*

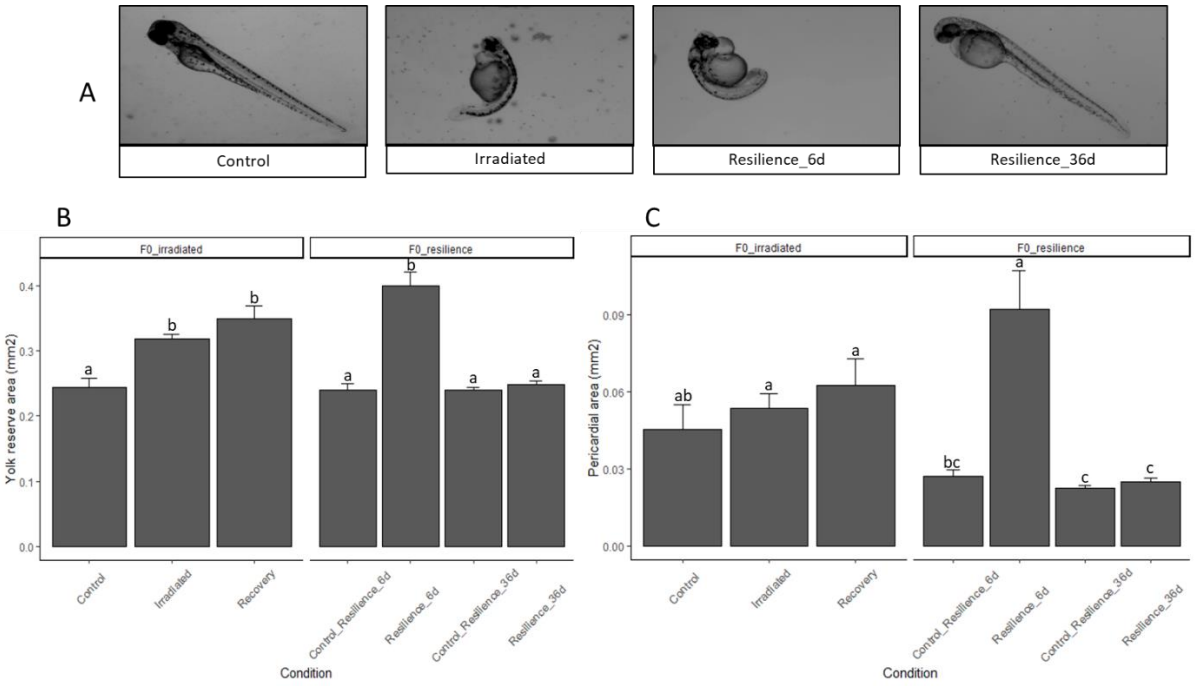

Figure 3: (A) Photographs of F1 larvae at 72 hpf after Control, F0 exposure to 50 mGy.h^{-1} (10 days) with F1 exposure to 50 mGy.h^{-1}(Irradiated), F0 exposure to 50 mGy.h^{-1} (10 days) follow by non-irradiation 6 days (Resilience_6d) or 36 days (Resilience_36d). (B and C) Bar plot of yolk reserve area (mm²) and pericardial area (mm²) for control (n=6), control_resilience_6d (n=11), control_resilience_36d (n=45), irradiated (F0 + F1 exposed to 50 mGy.h^{-1}, n=9), recovery (F0 exposed to 50 mGy.h^{-1}, F1 non-irradiated, n=12), resilience_6d (F0 exposed to 50 mGy.h^{-1} follow by non- irradiation exposure 6 days, F1 non-irradiated, n=11), resilience_36d (F0 exposed to 50 mGy.h^{-1} follow by non-exposure 36 days, F1 non-exposed, n=32). Letters indicate statistical differences (pl<0.05) among conditions (Anova test and Tukey post-hoc).

809

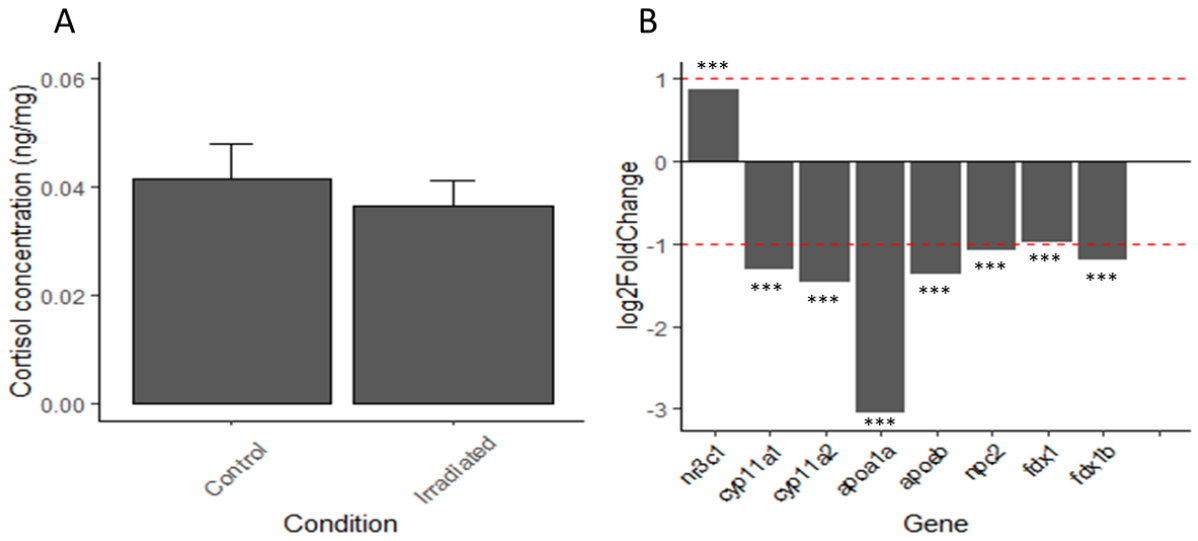

810

811 *Figure 4: (A) Bar plot of F0 ovaries cortisol concentration after control and exposure to 50 mGy.h^{-1} (irradiated), n=6*
812 *per condition. (B) Barplot of log2FoldChange (as compared to controls) for genes involved in cortisol metabolism;*
813 *n=8 per condition. Data came from transcriptomic data on F0 ovaries. Red line represents cut off value chosen for*
814 *interpretation of gene regulation. * ($p < 0.05$), ** ($p < 0.01$), *** ($p < 0.001$).*

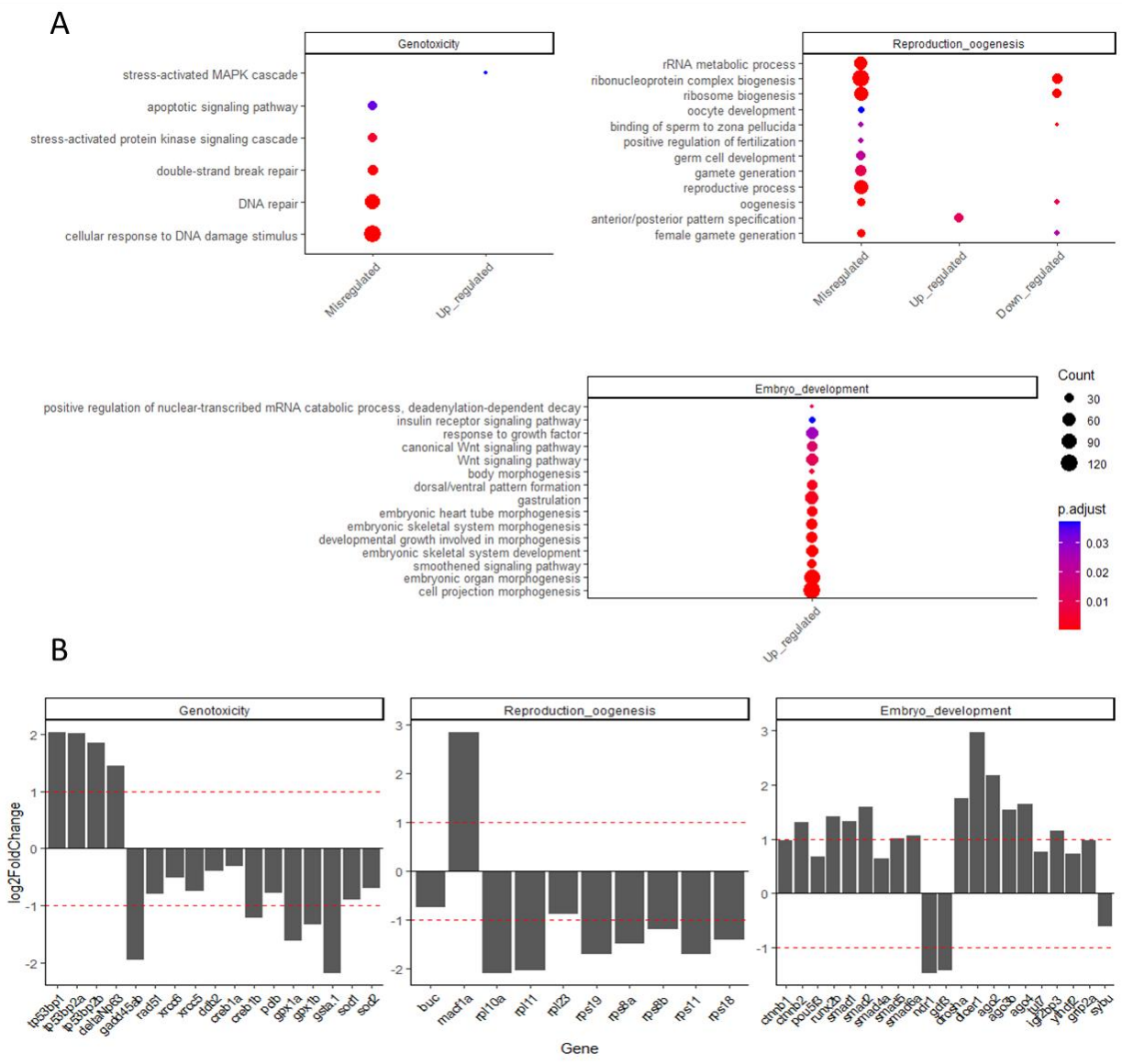

Figure 5: (A) Dot plot of selected GO (Gene Ontology) term enrichment from dysregulated, up and down genes in exposed F0 ovaries. Colours indicate the p-values from Fisher's exact test, and dots size is the number of genes constituting the given pathway. n=8 per condition. (B) Change in gene transcription levels (FC as compared to controls) in female gonad F0 from transcriptomic data. For all genes, FDR<0.01. Red line represents cut off value chosen for interpretation of gene regulation. n=8 per condition.

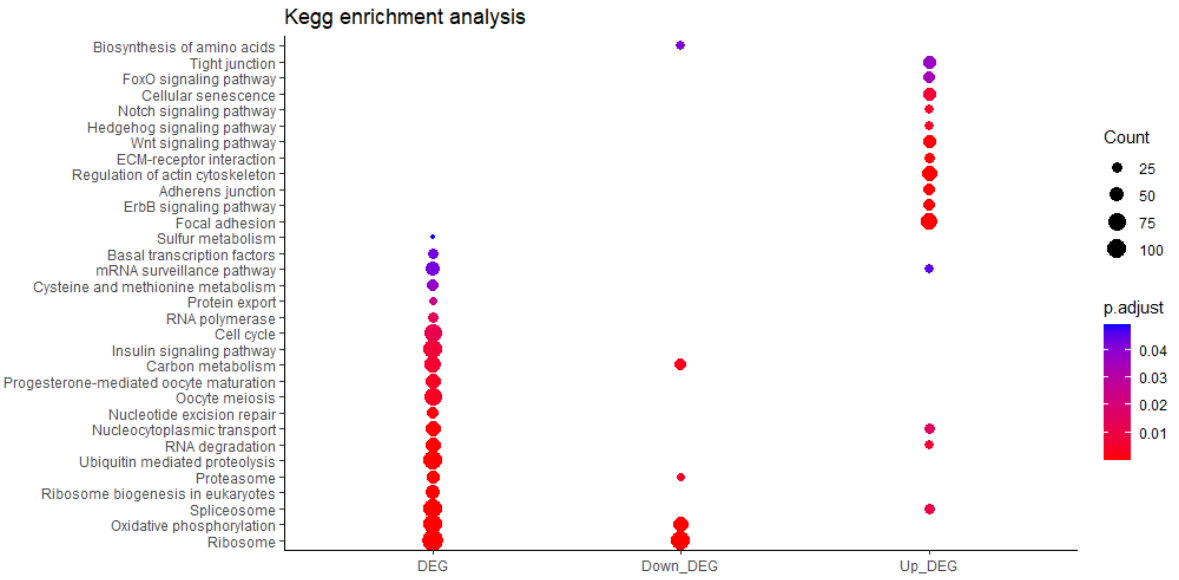

Figure 6: Dot plot of selected KEGG enrichment using human orthologues from misregulated, up and down genes in irradiated ovaries. Colours indicate the enrichment p-values from exact Fisher's test, and dots size is the number of genes constituting the given pathway. n=8 per condition.